Surface displacement monitoring and geophysical source modeling at the gas storage cavern field Epe

Alison SEIDEL[1,*], **Markus EVEN**[1], **Hansjörg KUTTERER**[1], and **Malte WESTERHAUS**[1]

[1] *Karlsruhe Institute for Technology, Karlsruhe, Germany (alison.seidel@kit.edu, markus.even@kit.edu, hansjoerg.kutterer@kit.edu, malte.westerhaus@kit.edu)*

[*] *corresponding author*

Abstract

The surface above gas storage caverns experiences strong and complex displacements often of a seasonal nature depending on the usage of the caverns. As the pressure inside a cavern is lower than in the surrounding rock the cavern converges continuously which leads to a subsidence bowl at the surface. Precise measurements with high spatial and temporal resolution of these displacements is important for monitoring the caverns but also for assessing potential risks for infrastructure in the area. Multitemporal SAR interferometry (InSAR) can produce dense spatial measurements of surface displacements. When jointly analyzed with GNSS and in situ measurements, accurate estimates of the 3D surface displacement field can be achieved. We measure and model surface displacements at Epe storage cavern field in North Rhine-Westphalia Germany with time series of up to 9 years of InSAR, GNSS and leveling data. The observed surface displacement caused by cavern convergence is partially superposed by other strong displacement effects such as the surface response to groundwater level changes. With statistical component methods we are able to separate these effects and create a geophysical source model to validate our measurements. With such a model, we can estimate future surface deformation and displacements at places without measurements based on a causal relation to the cavern usage. Our predicted displacements show a good agreement with InSAR time series, GNSS and leveling. Furthermore, we observe an additional displacement component over a fen that supposedly originates from changes of groundwater levels.

Keywords: storage caverns, 3D surface displacements, subsidence monitoring, geophysical model

1 Introduction

Storage caverns in salt-rock layers are an important part of the energy infrastructure. Gas and oil can be bought in summer and stored to be readily available when it is needed in winter, creating a seasonal cycle of filling levels. Cavern storages have the advantage of allowing rapid injection and withdrawal in higher quantities compared to pore storages, making their usage more flexible to the day-to-day demands in energy supply, but have the downside of progressing convergence, which limits the usage lifetime, as the cavern eventually will become unstable. This convergence is caused by the permanent lower pressure inside the caverns compared to the lithostatic pressure of the surrounding rock, even at high filling levels, and the viscoelastic behavior of the salt rock.

Usually, the volume loss inside the caverns also propagates through the overlying rock layers towards the surface, creating a subsidence bowl above the cavern, that can cause damage to infrastructure. The amount of convergence and subsequent surface subsidence is dependent on the local geological conditions, as well as cavern properties. Important properties include cavern size and shape, as well as temperature inside the cavern, depth of the cavern, and frequency and amount of injection and extraction of gas such as shown in studies such as Lyu et al. (2024) and Liu et al. (2019). The most influential parameter, as demonstrated in Xie et al. (2018), and Wang et al. (2014) is the pressure difference relative to the surrounding rock, which for gas caverns, varies with the filling level of the cavern. Monitoring the

progress of cavern convergence and surface subsidence, depending on the cavern usage is important to predict and prevent damage to infrastructure.

However, cavern volume measurements are usually only conducted every few years, so the temporal resolution of the data only allows for deriving long time trends. Cavern convergence can also be inferred from surface subsidence, but in order to determine the volume loss from displacements of the surface, a suitable geophysical model and good spatial and temporal sampling of measurements are needed, especially in cases where multiple caverns are in close proximity. Traditional geodetic methods such as leveling and GNSS, offer either only decent spatial coverage or high temporal resolution. Multitemporal (MT) InSAR provides both and can bring new insights on the spatiotemporal behavior of a displacement field, but has the downside of only measuring displacements in one dimension, the satellites line of sight (LOS). If tracks from different orbits are combined, vertical and east-west directed horizontal displacements can be estimated (Wright et al., 2004). Due to the near polar orbit of current SAR missions, the estimation of north-south component of displacement has a high standard deviation and cannot be determined reliably (Fuhrmann and Garthwaite, 2019). In terms of spatial coverage, MT-InSAR depends on consistency of stable backscattering characteristics of ground targets so it is dependent on local conditions.

To fully monitor and understand the spatiotemporal 3D displacement field in a multi cavern scenario, we propose an integrated approach based on InSAR and data provided by the operators. We derive a geophysical source model for the gas storage cavern field Epe that allows to predict surface subsidence based on filling levels of the gas caverns.

2 Epe cavern field

Epe, located in North Rhine-Westphalia, has currently the second largest storage capacity for natural gas in Germany. The 114 caverns, in depths of 1000-1500 m in Zechstein Werra rock salt layer (Axel Gillhaus, 2006), are owned by the company Salzgewinnungsgesellschaft Westfalen (SGW). More than 50 caverns are currently used for gas storage, and a few for oil storage, rented by different providers. The rest is used for brine production by SGW. Figure 1 shows the locations of the different types of caverns throughout Epe. Gas caverns are primarily located in the central and eastern part of the cavern field, while the liquid filled caverns are mostly in the western part of the field. The different types of caverns and differences between companies in operating the gas caverns, results in varying convergence behavior for the caverns in the field, causing a complex deformation regime on the surface.
Additionally, the western part of the cavern field is partly covered by a fen, where the surface is subject to strong seasonal displacements, that earlier studies (Even et al., 2022; Seidel et al., 2024), relate to groundwater levels in the fen. These displacements superpose with the signal caused by cavern shrinkage. A schematic overview of the main sources of displacement in Epe is shown in Figure 2.

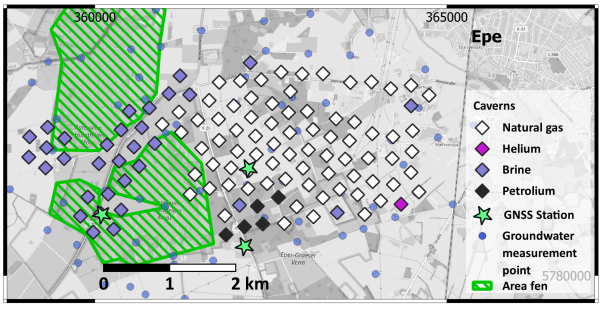

Figure 1. Map of the storage cavern field in Epe . Caverns of different types are indicated with diamonds, the fen area is marked with green dashed lines, locations of GNSS permanent stations are marked with green stars. From Seidel et al. (2024)

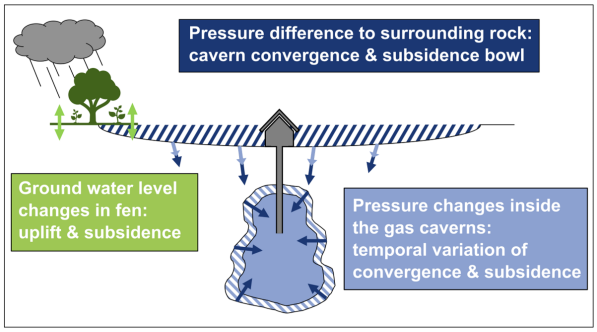

Figure 2. Schematic depiction of the main displacement sources in Epe cavern field. From Seidel et al. (2024)

3 Data

3.1 Surface displacement measurements

3.1.1 Leveling and GNSS

To monitor deformation in Epe, SGW holds annual leveling campaigns in spring to early summer, that cover more than 500 points along streets and facility areas through the entire field. For this contribution, leveling data from campaigns from 2015 to 2022 have been used. Additionally, SGW installed three GNSS permanent stations and a local reference station in 2018 (see Figure 3 for station locations), that provide hourly solutions. The station in the western field regrettably went out of commission due to vandalism in 2020. Also, the reference station is located so close to the field, that is is already slightly influenced by displacement, which affects the displacement solutions of all other stations. For this study, this effect has been corrected for east and vertical component by estimating a trend at the station from InSAR and adding it to all other station solutions.

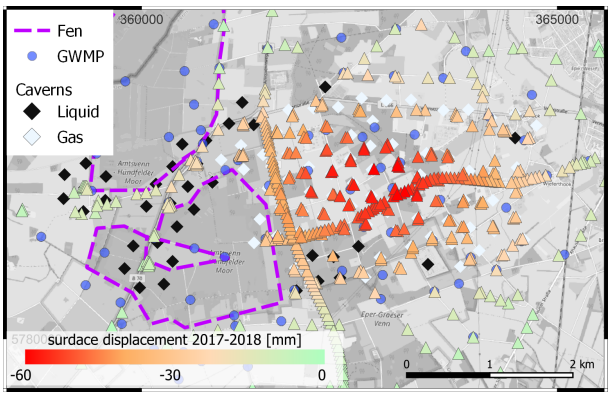

Figure 3. Difference in surface displacement measured between the leveling campaigns of summer 2017 to summer 2018 (triangles). Points where groundwater measurements are conducted are marked as blue circles

3.1.2 Multitemporal InSAR

We processed SAR data of the Sentinel-1 mission for the period April 2015 to December 2023. Four tracks with two viewing geometries from the ascending (asc. 15 and 88) and two from the descending (dsc. 37 and 139) flight direction were processed independently, using a combination of Persistent Scatterer (PS) and Distributed Scatterer (DS) processing, developed by Even (2019), to maximize the spatial coverage. All tracks are referenced to master scenes in February or March of 2019 and cover the entire cavern field.
The use of DS results in many scatterers in the fen area, where no GNSS or leveling measurements are available. Those scatterers primarily display the groundwater related displacement signal, but do also contain information about the cavern related signal. In this contribution we only discuss the results of track dsc. 37. For results on all four tracks and further details on the processing, see Seidel et al. (2024).

3.2 Supplemental data

SGW provided us with supplemental information for each cavern, consisting of coordinates, volume at the most recent sonar screen, depth of top and bottom of the salt rock layer, storage media and provider that rented the cavern. For all caverns operated by Uniper-Energy, the provider also supplied us with annual cavern volume data for all of their caverns. From AGSI (2024) we can obtain daily historical filling levels of the natural gas caverns for all providers in Epe since 2016, for some longer, as shown in Figure 4. For each provider, only the total filling level of all their caverns combined is available, not those of individual caverns. Filling levels of all providers show a similar annual cycle of injection in the summer and autumn months and depletion in the winter and spring months. Yet for some years and providers, levels can be very different. We do not have data on filling levels of the single helium cavern, nor for the oil caverns. SGW states that all Brine caverns are in the production phase. SGW also measures groundwater levels at several groundwater measurement points (GWMP) throughout the cavern field (see Figure 3). For most GWMPs, measurements are taken every two to three months, for a few, daily measurements are available, but only until 2018.

4 Measured surface displacements

All methods show a spatiotemporal complex displacement field above Epe. InSAR time series throughout the cavern field show very different displacement curves (Figure 5).

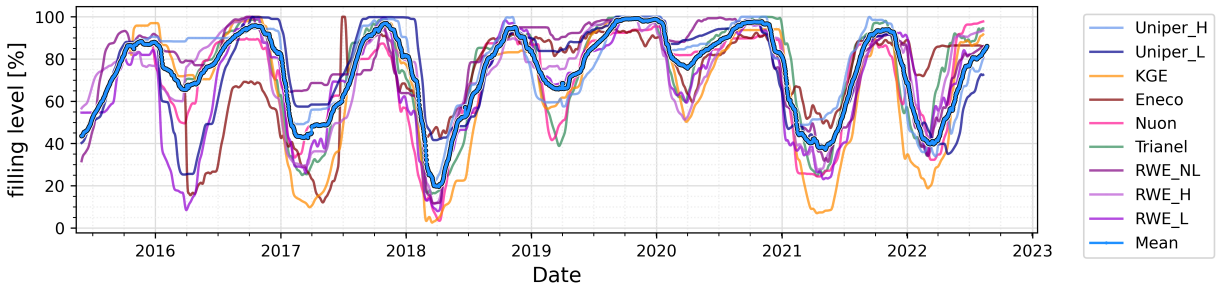

Figure 4. Gas cavern filling levels of all providers at Epe from AGSI (2024). From Seidel et al. (2024)

Though all time series display a negative trend that is stronger in the central cavern field, scatterers on the fen in the western field show a strong seasonal component with uplift and subsidence (purple star).

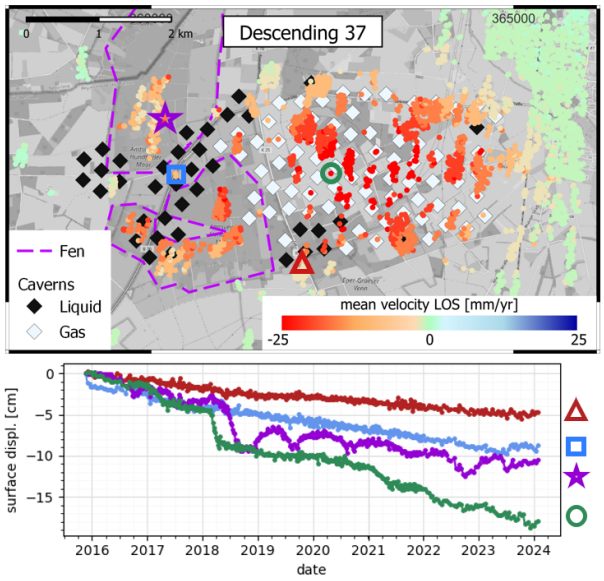

Figure 5. LOS displacements of InSAR Track dsc. 37, as mean velocities (top) and selected time series (bottom). The location of the scatterers for the displayed time series are marked with symbols in the map plot. Red Triangle: A scatterer in the southern field, where NS-directed displacement is assumed to be strongest; Blue square: A scatterer on a road above the liquid filled caverns in the western part of the cavern field; Purple star: A scatterer in the northern fen; Green circle: A scatterer in the center of the cavern field

The assumption of groundwater level changes as likely cause matches the minima in summer and maxima in autumn and winter. In contrast, the center field (green circle) also displays a cyclic trend,but only as annual variation of a negative displacement trend with maxima in summer and minima in winter. This can be attributed to the seasonal change in filling levels of the gas caverns, where convergence is always ongoing, but at different velocities. Time series on built infrastructure above groups of liquid filled caverns (red triangle and blue square) show mostly linear displacements, indicating that those caverns do not experience strong pressure changes that would cause varying rates of convergence.

Vertical displacements derived from InSAR and leveling and GNSS measurements show high consistency and prove that similar signal measurement qualities can be achieved, even at different spatial and temporal coverage and resolution.

The different signal contributions can be isolated and assigned to their source mechanism with statistic component source separation methods, as shown in Seidel et al. (2025). This allows the derivation of model time series for fen and gas cavern related signals independently, to serve as model to improve InSAR processing as described in Seidel et al. (2024). Furthermore, a separation of and removal of non cavern related signals aids the derivation of local parameters for a geophysical source model for cavern behavior from displacement measurements.

5 Cavern source model

5.1 Model parametrization

To achieve a better understanding of the full spatiotemporal displacement field of Epe, and to relate cavern operation to surface displacement, we aim to derive a model that gives a functional relationship

between cavern filling levels that are publicly available at AGSI (2024) at a very high temporal resolution, and surface displacement. Such a model then allows for estimations of displacement at places or points in time where no measurements are available, and enables predictions on how surface displacements would develop, depending on different cavern usage scenarios. A highly accurate model would require a of of additional information, such as the exact shape and size of every cavern, temperature and pressure distribution at the caverns and the exact rheological properties of the salt rock and the overlying rock layers. Many of these are unknown or not available to us and have to be approximated. Hence we will derive a model based only on the limited information available to us and investigate its accuracy. Our model consists of two steps. First, filling levels are related to cavern volume loss. Second, the propagation of volume loss to the surface is predicted.

5.2 Cavern convergence

Caverns converge depending on the amount of stress that they experience. Therefore, for accurate geophysical description of cavern convergence, the exact pressure levels inside the caverns would be required, which are usually not made public by the cavern operators. For gas caverns, pressure levels can be calculated from filling levels, if maximum (100%) and minimum (0%) allowed pressure inside a cavern are known. One of the operators provided these numbers to us.

We use the Norton creep law (Equation 1, given in Ślizowski et al. (2010) for relating the difference between the pressure inside the cavern p_{cav} and the lithostatic pressure p_{lith} to cavern volume loss $\frac{dV}{dt}$.

$$\frac{dV}{dt} = A \cdot e^{-(\frac{Q}{R \cdot T})} \cdot (p_{cav} - p_{lith})^n \qquad (1)$$

T is the temperature inside the cavern, Q is the activation energy of the salt and R is the Boltzmann constant. The creep rate coefficient A and the stress exponent n, are local material parameters. We use literature values for Q, as given in Ślizowski et al. (2010), and assume a constant value of 40°C for T as we have no information on the actual temperature gradient. To calculate the lithostatic pressure at the depth of the center of each cavern, we assume for the rock layers above the salt layer a density of $2.6 g/cm^3$ and for the salt layer a density of $2.2 g/cm^3$.

In order to be able to calculate the volume changes for an individual cavern based on the cavern pressure with help of Equation 1, we need the parameters n and A. To determine them, we fit with help of the simplicial homology global optimization (shgo) algorithm by Endres et al. (2018) the prediction obtained by Equation 1 to the annual cavern volume measurement data provided by Uniper Energy (cp. Figure 6). This way, we obtained no unambiguous solution (n,A). The set of pairs (n,A) that give a good prediction for the annual convergence can be described by an exponential relation between the two variables. If it is assumed in addition that surface displacements at the center of the cavern field are proportional to volume changes and fit the prediction of the volume model to this time series, values $(n,A) = (5.8,\ 0.0038)$ are found.

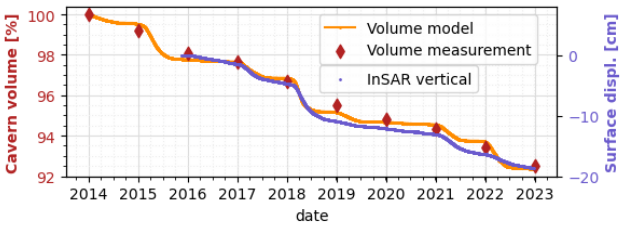

Figure 6. Model predicted cavern volume curve (yellow line) and actual cavern volumes from 2014 to 2023. The purple line shows vertical surface displacements from InSAR time series at the center of the cavern field.

We calculate historical volumes from 2014 to 2024, based on the one volume measurement we have for each cavern, for all gas caverns depending on the filling levels of the provider that rents it. For liquid filled caverns, we use a linear convergence model with convergence rates defined in Sroka et al. (2017). For the Helium filled cavern and for all providers where no data is available from 2014-2016, we calculate mean filling levels from all other providers, weighted by the storage capacity each provider has in Epe, and use this mean curve as substitute (see Figure 4, blue curve).

5.3 Surface displacements

To describe the surface displacements as a function of cavern volume loss, we use the Sroka-Schober model (Sroka et al., 2017), based on the work of Sroka (1982), in a multi cavern scenario, as in Even et al. (2022) for Epe, where the displacements of all caverns superpose each other. The maximum subsidence caused by the volume loss $\Delta V(t)$ of one cylindrical cavern d_{max} is described through Equation 2, where H_{top} and H_{bot} are the depths of the cavern roof and floor, and β is the angle of main influences (Knothe, 1953), see Figure 7 for reference. α is the coefficient of volume loss, i.e. the ratio between the volume change in the subsidence trough at the surface and the volume change in the cavern.

$$d_{max}(t) = \frac{\alpha \cdot \Delta V(t)}{H_{top} \cdot H_{bot}} \tan^2 \beta \tag{2}$$

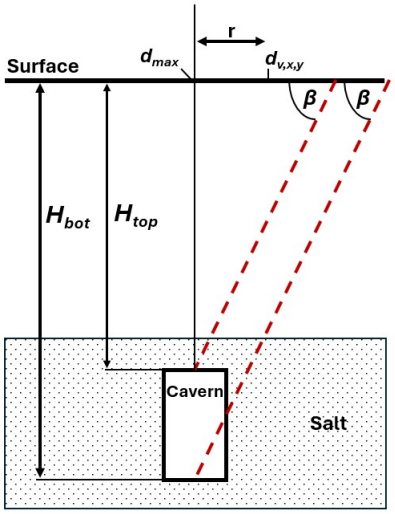

Figure 7. Sroka-Schober model of a cavern. β is the angle of main influences, H_{top} and H_{bot} are the depths from surface to cavern roof and floor, r is the distance of a certain point from the point of maximum subsidence d_{max}.

Vertical displacements $d_v(r,t)$ at a certain distance to the cavern $r = \sqrt{x_{dist} + y_{dist}}$ are then described by Equation 3. For horizontal displacements $d_x(r,t)$ and $d_y(r,t)$ Sroka et al. (2017) follow Awierszyn (1947) who states that the horizontal displacement for a single cavern has a linear relationship with the vertical displacement, as in Equation 4. It is dependent on the horizontal movement factor B and the Tilt-Vectors T_x, T_y.

$$d_v(r,t) = d_{max}(t) \cdot e^{\left(-\pi \frac{r^2}{H_{top} \cdot H_{bot}} \cdot \tan^2 \beta\right)} \tag{3}$$

$$d_x(r,t), d_y(r,t) = -B \cdot T_{x,y} \tag{4}$$

$$T_x = \frac{-2\pi}{(H_{top} \cdot H_{bot})} \cdot \tan^2 \beta \cdot x_{dist} \cdot d_v(r,t) \tag{5}$$

$$T_y = \frac{-2\pi}{(H_{top} \cdot H_{bot})} \cdot \tan^2 \beta \cdot y_{dist} \cdot d_v(r,t) \tag{6}$$

We model all caverns as cylinders and estimate cavern floor and roof depths from their volume, assuming a cavern radius of 40 m for all caverns. B and β have been estimated by Even et al. (2022) and Sroka et al. (2017) for Epe before. For now, we use $B = 700m$ and $\beta = 30°$, which are the mean values estimated by Even et al. (2022) for both of their parameters. Both sources also model surface displacements for a multi-cavern scenario for Epe, but only for linear convergence rates (Sroka et al., 2017) or for a model that parametrizes convergence as a combination of a linear trend and a pressure driven component Even et al. (2022). Different than them, we use the estimated cavern volume loss from Equation 1, with a temporal resolution of 1 day to calculate surface displacements of the same temporal resolution. To compare the model output with InSAR, we also transform the predicted displacements to the LOS-vectors of the different tracks, as described in Wright et al. (2004).

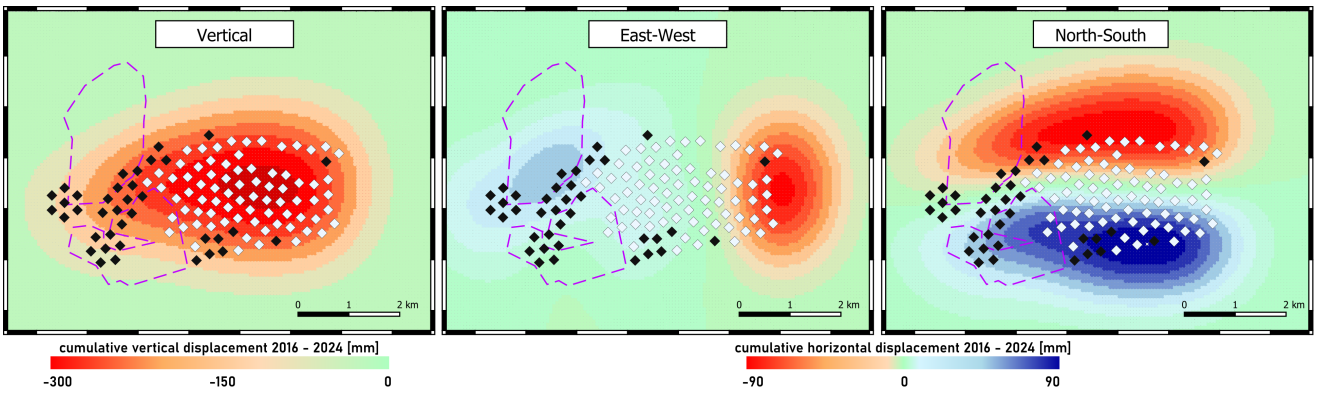

Figure 8. Modeled horizontal and vertical displacement components. The caverns (diamonds: black are liquid filled caverns, white are gas caverns) and the shape of the fen (dashed purple line) are added for orientation.

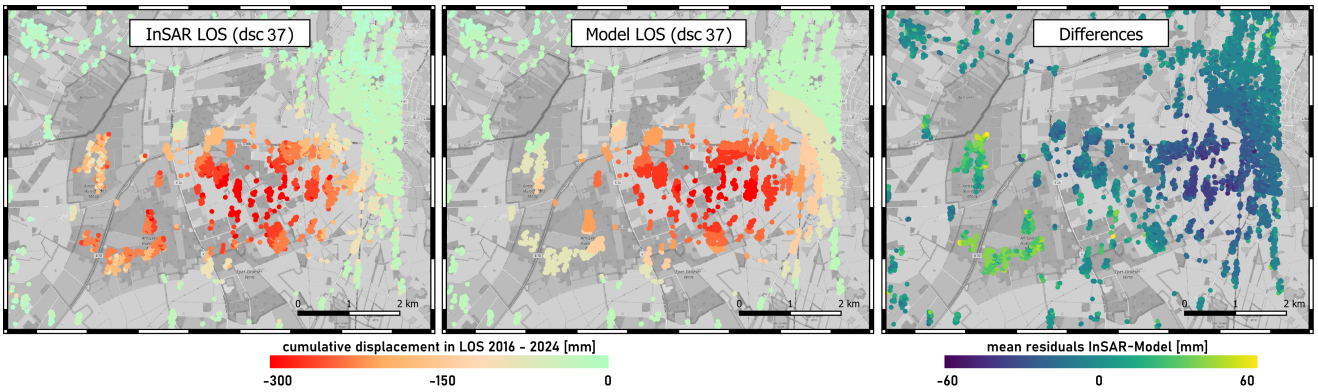

Figure 9. Cumulative displacement from 2016 to 2024 estimated from InSAR time series (left), and model (center) in LOS of track dsc. 37. The mean residual (of all points in time) for each scatterer between model and InSAR is displayed on the right.

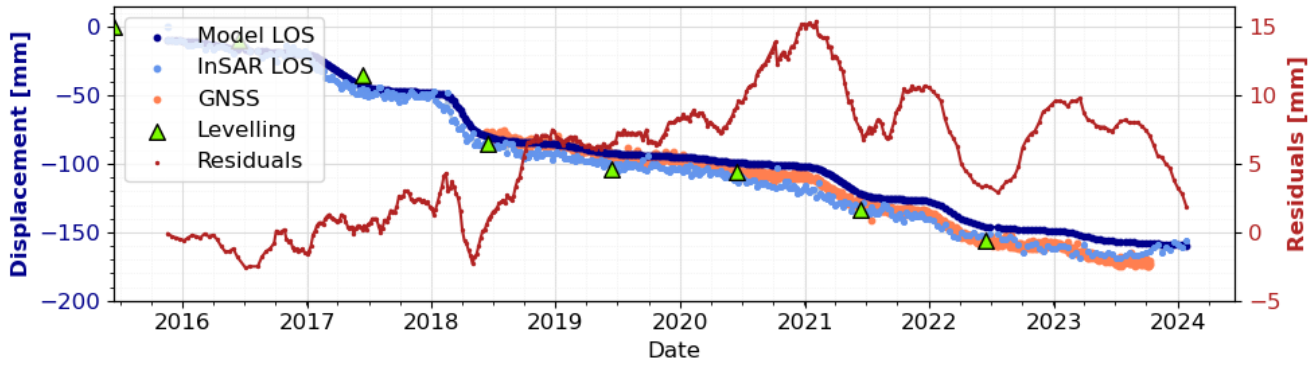

Figure 10. Comparison of modeled deformation translated to LOS geometry of dsc. 37 (dark blue) with results of InSAR time series analysis of track dsc. 37 (light blue), GNSS (orange) and leveling measurements (green triangles), also translated to LOS, in the center of the cavern field. Left y-axis displays ground displacement [mm] in LOS, right y-axis represents the residuals (red) between model and InSAR time series [mm] in LOS.

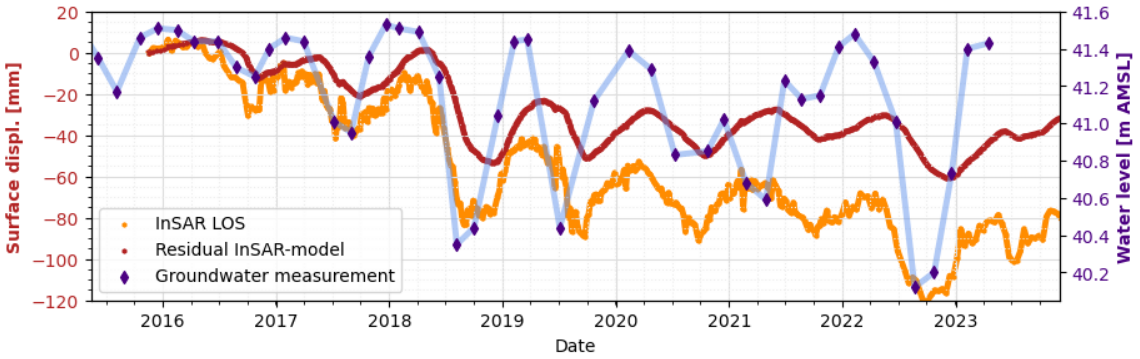

Figure 11. InSAR time series of track dsc. 37 (orange) of surface displacements of a scatterer in the northern fen, and groundwater level measurements close to the scatterer, as well as residuals of InSAR and model (red). Here, residuals and InSAR measurements are on the same scale.

6 Discussion of the model results

Even though our model relies on many assumptions and approximations, preliminary results already seem to describe the spatiotemporal displacement field reasonably well. The modeled cumulative vertical displacements (Figure 8) show a slightly elongated subsidence trough with maximum displacements of 30 cm over eight years at the center of the gas cavern field. East-West directed horizontal displacements show asymmetrically shaped extrema, where the maximum of westward directed displacements is larger than eastward directed displacements, which can be attributed to the spatial distribution of the caverns, and also the distribution of the different types of caverns. The north-south directed horizontal displacements again display a more regular spatial pattern that would be expected for a subsidence trough.

When we project the model results to the LOS-vector of track dsc. 37 and compare them with the InSAR measurements of this orbit (Figure 9), we find the largest residuals in the area of the fen, which is expected, as the model does not describe the displacements caused by changes of groundwater level here. We also find larger residuals at the eastern end of the cavern field, where the model predicts the maximum of westwards directed displacements. We assume that the model overestimates the horizontal displacements, which could be attributed to a too large horizontal movement factor B. This would also cause an overestimation in north-south directed displacements. Even though there are no strong residuals in the area of the extrema of the north-south directed displacements, this can be explained by the insensitivity of the LOS-vector to these displacements.

Time series in the center of the cavern field (Figure 10) show a very good agreement between model and geodetic measurements, especially in terms of temporal shape of the displacement curve. In total, the model underestimates the negative displacement here slightly. This could be attributed to a slightly too small angle of main influences β. A small temporal delay is also visible between InSAR and model, which is also expected, due to the delayed viscoelastic response of salt rock, which is not yet considered in this model.

The comparison of time series for scatterers in the fen with groundwater measurements confirms the assumption that these displacements are mainly related to changes of groundwater levels (Figure 11). Only a slight subsidence trend from the InSAR time series is explained by model. The residuals curve is very similar to the water levels, but still contains negative trend. This could indicate that the fen is drying up and losing material, which would cause subsidence, but it could also mean that the assumed linear convergence trend for liquid filled caverns is too small.

7 Conclusions and Outlook

The geodetic measurements at Epe cavern field show a complex deformation regime that can not be

fully described with data from one method alone. Multitemporal InSAR offers the best combination of spatial coverage and temporal resolution. With a geophysical source model surface displacements can be obtained from gas cavern filling levels, using model parameters derived from the displacement measurements.

The use of the Norton creep law for a temporal high resolution model of cavern convergence looks promising. The accuracy of the convergence estimates could be improved with actual cavern pressure data that are recorded by the providers. The Sroka-Schober model has been used for describing cavern related displacements at Epe before in Sroka et al. (2017) and Even et al. (2022). First results with the parameter values from Even et al. (2022) look promising, where displacements in the central cavern field are slightly underestimated and horizontal displacements overestimated. However, their results rely on a parametrization of convergence to a linear trend and a cyclic signal and was derived from a shorter time series of three years. Sroka et al. (2017) find larger local parameter values than Even et al. (2022) for β and relate B to individual cavern depths and β, resulting for most caverns in a smaller B than in Even et al. (2022). An increase of β would create a smaller area of influence for each cavern and therefore stronger displacements inside this area. A smaller B on other hand would decrease horizontal displacements, which our model currently overestimates.

To improve the model predictions, future work will focus on deriving the local parameters for B and β for the Sroka-Schober-model ourselves, and do a combined optimization using all available geodetic measurement data for Epe. This optimization will then also derive the optimal parameter pair of n and A and consider the viscoelastic properties of the salt rock by including a relaxation time in the model. For this we could utilize a basic Kelvin-Voigt body as in Even et al. (2020).

With such an improved model, we expect to obtain more accurate results for Epe. Furthermore, we intend to investigate the applicability of this model for other cavern fields with similar geological settings.

Acknowledgments

We would like to thank Stefan Meyer from SGW (Salzgewinnungsgesellschaft Westfalen) for providing the GNSS and leveling data, as well as the groundwater measurement data for Epe. We are grateful to Uniper Energy GmbH storage for providing additional data and information about their caverns in Epe. We also thank the German Federal Ministry of Economics and Climate Protection for funding this work as part of the DGMK project 867 SAMUH2.

References

AGSI (2024). Aggregated gas storage inventory. `https://agsi.gie.eu/#/`. Last checked on Jan 30, 2025.

Awierszyn, S. G. (1947). *Mining subsidence engineering*. Ugletiechizdat.

Axel Gillhaus, Fritz Crotogino, D. A. (2006). Compilation and evaluation of bedded salt deposit and bedded salt cavern characteristics important to successful cavern sealing and abandonment. Technical report, Solution Mining Research Institute.

Endres, S. C., Sandrock, C., and Focke, W. W. (2018). A simplicial homology algorithm for lipschitz optimisation. *Journal of Global Optimization*, 72(2):181–217.

Even, M. (2019). Adapting stamps for jointly processing distributed scatterers and persistent scatterers. In *IGARSS 2019 - 2019 IEEE International Geoscience and Remote Sensing Symposium*. IEEE.

Even, M., Westerhaus, M., and Seidel, A. (2022). Konvergenz- und druckabhängige oberflächenverschiebungen über einem kavernenspeicherfeld in nw-deutschland, beobachtet mit methoden der radarinterferometrie. *DGMK/ÖGEW Frühjahrstagung 2022 – Geo-Energy-Systems and Subsurface Technologies – Key Elements towards a Low Carbon World*, pages 33–41.

Even, M., Westerhaus, M., and Simon, V. (2020). Complex surface displacements above the storage cavern field at epe, nw-germany, observed by multi-temporal sar-interferometry. *Remote Sensing*, 12(20):3348.

Fuhrmann, T. and Garthwaite, M. C. (2019). Resolving three-dimensional surface motion with

InSAR: Constraints from multi-geometry data fusion. *Remote Sens. (Basel)*, 11(3):241.

Knothe, S. (1953). Równanie profilu ostatecznie wykształconej niecki osiadania. *Archiwum Górnictwa i Hutnictwa*, 1(1):22–38.

Liu, H., Zhang, M., Liu, M., and Cao, L. (2019). Influence of natural gas thermodynamic characteristics on stability of salt cavern gas storage. *IOP Conference Series: Earth and Environmental Science*, 227:042021.

Lyu, C., Dai, H., Ma, C., Zhou, P., Zhao, C., Xu, D., Zhang, L., and Liang, C. (2024). Prediction model for three-dimensional surface subsidence of salt cavern storage with different shapes. *Energy*, 297:131265.

Seidel, A., Even, M., Kutterer, H., and Westerhaus, M. (2024). Monitoring eight years of surface displacements at the storage cavern field epe with multitemporal insar. *avn – allgemeine vermessungs-nachrichten*, (5):270–280.

Seidel, A., Westerhaus, M., Even, M., and Kutterer, H. (2025). Signal decomposition with insar displacement time series above a storage cavern field: Example epe (nrw, germany). *International Association of Geodesy Symposia*.

Sroka, A., Misa, R., Tajduś, K., Klaus, M., Stefan Meyer, S., and Feldhaus, B. (2017). Forecast of rock mass and ground surface movements caused by the convergence of salt caverns for storage of liquid and gaseous energy carriers.

Sroka, A.; Schober, F. (1982). Die berechnung der maximalen bodenbewegungen über kavernenartigen hohlräumen unter berücksichtigung der hohlraumgeometrie. *Kali Steinsalz*, 4:273–277.

Wang, T., Yang, C., Yan, X., Li, Y., Liu, W., Liang, C., and Li, J. (2014). Dynamic response of underground gas storage salt cavern under seismic loads. *Tunn. Undergr. Space Technol.*, 43:241–252.

Wright, T. J., Parsons, B. E., and Lu, Z. (2004). Toward mapping surface deformation in three dimensions using InSAR. *Geophys. Res. Lett.*, 31(1).

Xie, P., Wen, H., and Wang, G. (2018). An analytical solution of stress distribution around underground gas storage cavern in bedded salt rock. *J. Renew. Sustain. Energy*, 10(3):034101.

Ślizowski, J., Urbańczyk, K., and Serbin, K. (2010). Numerical analyses of gas storage caverns convergence in salt dome; [numeryczna analiza konwergencji pola komór magazynowych gazu w wysadzie solnym]. *Gospodarka Surowcami Mineralnymi / Mineral Resources Management*, 26(3):85–93.